KINETICS OF DISCONTINUOUS PRECIPITATION AND DISSOLUTION IN Cu–4.9 at % Sb ALLOY

A Thesis Submitted
In Partial Fulfilment of the Requirements
for the Degree of

MASTER OF TECHNOLOGY

BY

SOMONNOY GHOSH

to the

DEPARTMENT OF METALLURGICAL ENGINEERING

INDIAN INSTITUTE OF TECHNOLOGY KANPUR

APRIL, 1992

CERTIFICATE

This is to certify that the thesis entitled '**Kinetics of Discontinuous Precipitation and Dissolution in a Cu-4.9%Sb Alloy**' is a bonafide record of work done by **Shri Somonnoy Ghosh**, in partial fulfilment of the requirements of M.Tech. degree, under my supervision and has not been submitted elsewhere for the award of a degree.

(Dr. S. P. Gupta)
Deptt. of Metallurgical Engineering
Indian Institute of Technology
Kanpur

ACKNOWLEDGEMENT

I take this opportunity to express my heartfelt gratitude to Dr. S. P. Gupta for not only directing and supervising my work but also for his invaluable help at times of crisis.

I am indebted to Mr. K. P. Mukherjee who was ever ready to volunteer help, to Mr. B. K. Jain who facilitated the sample cutting, Mr. Pal who so painstakingly helped in taking the SEM photographs, and Mr. Srivastava and Mr. Murli who never made me hesitate to ask for assistance.

I am thankful to Mr. Yash Pal for typing the manuscript.

Thanks are due to Mr. A. K. Srivastava and Mr. Sudipto Ghosh who have been true friends and have stood by my side whenever I have needed them. Finally, a special mention or two: my parents and Rishi who have always had more confidence on me than I have myself, and to Jo whose smile has always given me hope.

CONTENTS

LIST OF SYMBOLS

δg_{PPT}	Driving force for reaction initiation following precipitation
ΔG_{GB}	Driving force for grain growth
ΔG_{def}	Driving force for recrystallization
ΔG_c	Chemical free energy change
ν	Growth rate
D_v	Volume diffusivity
D_b	Boundary diffusivity
k	Segregation ratio
δ	Grain boundary thickness
S^α	Thickness of α lamella
S^ε	Thickness of ε lamella
S	Interlamellar spacing
$^1X_B^\alpha$	Original alloy composition
X_B^ε	Composition of ε phase
$^pX_B^\alpha$	Depleted matrix composition
$^eX_B^\alpha$	Depleted matrix composition as given by equilibrium solvus
M	Grain boundary mobility
γ	Specific surface energy of α/ε interface
ΔG_1	Driving force used for primary cell growth
ΔG^ε	Free energy of formation of ε phase
L	Interaction parameter
$\Delta G_1^{\alpha+\varepsilon}$	Free energy of the $\alpha+\varepsilon$ phase mixture
N	Fraction of supersaturation recovered during reaction
ΔG^α	Available driving force for dissolution
ΔG_d^c	Chemical driving force for dissolution
ΔX_B^α	Difference between the recovered solute composition after dissolution and the solute composition in depleted α matrix in contact with ε in the original lamellar structure.

LIST OF TABLES

LIST OF FIGURES

ABSTRACT

The growth kinetics of the cellular precipitate has been studied in a Cu-4.9 at% Sb alloy in the temperature range 520-630K using optical microscopy and X-ray diffraction. The alloy was observed to completely decompose by cellular precipitation reaction into a lamellar aggregate of α and ε phases at all aging temperataures. Lattice parameter measurements indicated that the depleted matrix was richer in solute than the equilibrium solvus composition. Analysis of the growth kinetics of the primary reaction indicated that the transformation is controlled by diffusion of Sb through the cell boundaries.

Dissolution of the cellular precipitate has been studied in the same alloy in the temperature range 650-730K. Microstructural observations have revealed that the process of dissolution begins at the original position of the grain boundary. The steady state rate of cell boundary migration decreased with decreasing temperataure of dissolution. The boundary diffusivities have been estimated at a number of temperataures using the theory of Petermann and Hornbogen modified for dissolution. From the temperature dependence of the diffusivity, an activation energy of 136 kJ mol^{-1} is obtained. From the diffusivity and activation energy values, it may be concluded that the diffusion of Sb along the migrating grain boundaries countrols the process of dissolution in this alloy.

CHAPTER 1

INTRODUCTION

1.1 DISCONTINUOUS PRECIPITATION

This transformation, which has been studied in a number of alloy systems, is characterized by the decomposition of a supersaturated solid solution α^s into the solute rich precipitate phase ε embedded in the solute depleted phase α which is structurally similar to the super saturated α^s. This category of transformation has been termed as 'discontinuous precipitation', 'cellular reaction', 'the grain boundary reaction' and the recrystallization reaction. The solute rich phase ε nucleates at the grain boundary in the form of plates and the lamellar morphology of the products, ε and α, grows by the grain boundary migration across the supersaturated α^s phase. The term discontinuous is used because it can be shown experimentally that there is both a discontinuous change in orientation and a discontinuous change in solute composition across the advancing reaction front. These two factors distinguish discontinuous precipitation from other heterogeneous and homogeneous reactions giving morphologically similar products, such as those in which the surrounding matrix is continuously depleted of excess solute but there is no grain boundary migration, e.g. Ti-Cr (1), Fe-Sn (2), or those in which there is boundary migration but no change in composition, e.g. ordering in Ni_2V (3). This transformation, as mentioned earlier, is also frequently termed as cellular because the reaction product is an aggregate of alternate lamellae of α and ε in the form of cells just as in eutectoid reaction. It should be noted that many of the theoretical concepts derived for

the growth of a eutectoid reaction are also appropriate to any discontinuous reaction.

Hornbogen (4) has shown six different discontinuous -type reactions, which comprise such varying transfrormations as recrystallization and crystallization from the amorphous state. However, all the major grain boundary discontinuous reactions are encompassed by a nomenclature used by Thompson (5). Three major reaction types may be identified, the first being:

$$\text{Type 1} \qquad \alpha^{s} \longrightarrow \alpha + \varepsilon \qquad (1.1)$$

in which a single phase supersaturated matrix α^{s} transforms behind a moving grain boundary to alternate lamellae of the thermodynamically more stable mixture of ε precipipitate and solute-depleted α. The characteristic that there is no change in the crystal structure of α distinguishes discontinuous reactions from the morphologically similar eutectoid reactions. The present investigation is a type 1 reaction and may be described essentially as grain boundary precipitation with concurrent boundary migration.

Most of the alloy systems studied in the literature undergo type 1 reaction and hence the other two types are only briefly mentioned below.

The second type of reaction is

$$\text{Type 2} \qquad \alpha^{s} + \gamma \longrightarrow \alpha + \gamma \qquad (1.2)$$

wherein γ is a prior coherent matrix precipitate which transforms to coarser γ lamellae.

And the third type of discontinuous reaction is

Type 3 $\alpha^s + \gamma \longrightarrow \alpha + \varepsilon$ (1.3)

in which the coherent metastable γ changes to the thermodynamically more stable ε phase.

According to Williams and Butler (6) the discontinuous precipitation reaction generally has a deleterious effect on mechanical and physical properties. This is most evident in type 2 and 3 reactions in which the prior matrix coherent precipitates are responsible for age hardening of a wide range of alloys. The age hardening response is directly related to the size and distribution of these precipitates and the properties are invariably lost when overaging occurs. Such alloys form the basis of most high temperature materials applications in the form of Ni and Co base superalloys (7). Similarly, low temperature structural materials such as Al and Cu base alloys rely on age hardening for the strength required in their commercial applications. It is discontinuous precipitation which causes overaging in such alloys.

It should be noted, however, that the discontinuous reaction may have positive effects in certain circumstances. For example, Hornbogen (4) has proposed that directional discontinuous transformation may give rise to superior strengthening in comparison to eutectoids, since discontinuous precipitate lamellae have a smaller spacing. Also, repeated thermal cycling of iniation and dissolution may be usefully manipulated to give a dramatic refinement of grain size in a material.

1.2 OCCURENCE OF REACTION

A question which naturally comes to mind is whether the alloy

systems exhibiting this type of reaction have any characteristic property which distinguish these from the others not undergoing this transformation. An early suggestion concerning why the reaction occurs in some systems and not in others was that a minimum particle/matrix misfit parameter of ~1% was necessary for the reaction to occur. This implies that matrix strain energy is a major driving force for the reaction. However, observation of reactions in Ni-Ti (8), Ni-Al (9), and Al-Li (10) lend no suport to this rather simple idea. Bohm (11) used more successfully the concept of atomic mismatch, i.e. the difference in solvent/solute atomic sizes, as a necessary criterion for the reaction occurence in Cu-base alloys. An atomic mismatch > ~11% is stated to be the criterion. However, even this rule is not entirely accurate since Phillips (12) has reported the existence of a discontinuous reaction in Cu-Co alloys.

Meyrick (13) in an attempt to quantify the occurence of the reaction considered a circular segment of grain boundary, pinned at points separated by a length 2r, bulging forward a distance x under the driving force of the reaction which has its origin in the change of grain boundary energy with degree of solute

segregation. According to him for discontinuous precipitation to occur:

$$-\frac{\partial\gamma}{\partial X_B} > \frac{2x\gamma}{({}^1X_B^\alpha - X_B^\alpha)\, r^2} \qquad (1.4)$$

where $-\partial\gamma/\partial X_B$ is the rate of decrease of grain boundary energy with increase in the concentration X_B of the solute at the boundary, and ${}^1X_B^\alpha$ and X_B^α are the initial and final concentrations, respectively, of the area swept out by the boundary. The occurence or otherwise of the reaction depends on the segregation of solute atoms, which appears to bear some relation to the atomic misfit. Serious doubts on the ability of the Meyrick criterion to predict dis ontinuous precipitation have been cast by Plichta et al. (14) ho evaluated the occurence in Ti-X alloys and re-examined its presence in Cu-X alloys by relating grain boundary segregation to the maximum solubility limit. No correlation was found.

It may be safely concluded that the formulation of simple models cannot successfully predict the occurence of discontinuous precipitation. Therefore, because of the large number of factors that influence the various events required for discontinuous precipitation to occur, any simple single rule capable of predicting the occurence of this reaction is certain to have exceptions.

1.3 INITIATION OF REACTION

The initiation of the discontinuous precipitation reaction means the simultaneous occurence of two events, namely, the

occurence of heterogeneous grain boundary precipitation and the movement of the grain boundary. An increasing number of experimental studies have shown that these two processes are affected by the structure of individual boundaries. The various theories and observations that account for reaction initiation emphasize on what driving force causes the boundary to move initially and not the boundary structure. Structure-property investigations of grain boundaries have indicated relationships between grain boundary misorientation and boundary energy, diffusivity, impurity segregation level, and step density and mobility. Precipitation on grain boundaries has been shown to be influenced by the inclination and misorientation of the boundary, the orientation of the boundary plane vis-a-vis the habit plane of the precipitate, and the existence of grain boundary steps and ledges. It is the existence of these factors that explain the commonly observed phenomenon that the distribution of precipitates in an aged alloy varies widely from one grain boundary to another.

Smith (15) has noted that discontinous reactions do not occur on twin boundaries. Since it is well established that the nucleation of precipitates on grain boundaries is sensitive to boundary orientation, an absence of the discontinuous reaction on twins, where there is a perfect-coincidence relationship, is to be expected. Not only do the twins have low energies, their mobility is highly restricted by their coherency. The reaction was observed to occur at all boundaries if the aging time was sufficient and this clearly indicates that the boundary structure is an important parameter in the control of nucleation kinetics, though the effect of structure is not simple.

The influence of grain boundary structure on the discontinuous reaction has been investigated in a systematic way via the production, in an alloy system normally suspectible to the reaction (Cu-In), of bicrystals of known and predetermined mis-orientations (16). This approach has successfully explained how grain boundary structure affects precipitate densities and morphologies.

In precipitate-induced boundary migration, grain boundary precipitation is seen as essential in causing boundary deflection and thus initiation of the discontinuous reaction and it is implicitly assumed that the boundary would effectively be immobile in the absence of this precipitation.

The Tu and Turnbull 'pucker' mechanism (17) for discontinuous precipitate initiation begins with the nucleation, on one side of the grain boundary, of a disc or plate-shaped precipitate having a high-energy interface across the grain boundary and a low-energy interface with the grain in which it is embedded. The interfacial energy imbalance between the two broad faces of the precipitate causes the boundary to sweep the high-energy interface leaving the precipitate completely embedded in the grain but attached to the boundary at its tip. The boundary on one side of the precipitate is now favourably oriented for the nucleation of the second particle of the same orientation as the first, and the process repeats itself to build up a series of parallel plates which carry the boundary along as they migrate forward fed by boundary diffusion of solute. The driving force for boundary migration is thus provided by the reduction in the total interfacial energy of the precipitate.

The other extreme of initiation mechanism is precipitation on boundaries moving under some other driving force. The proponents of this approach to initiation, Fournelle and Clark (18), assume grain boundary migration as a precondition for nucleation to occur. Small thermally activated movements of the grain boundary are assumed to be possible in the absence of precipitation and these are sufficient to stimulate the formation of a cell nucleus, if boundary precipitation occurs concurrently. A clear distinction between this mechanism and that of Tu and Turnbull is that the precipitate/matrix orientation habit plane is of little importance. The migration of a grain boundary in the absence of precipitation is expected at high aging temperatures where normal recrystallization and grain growth tendencies occur. It is assumed by Fournelle and Clark (18) that a slight curvature in the α^s/α^s boundary provides a driving force for initial migration by a short distance. At this point, accumulation of solute at the boundary causes grain boundary allotriomorphs to form. Further migration of the boundary in the same direction is now possible because of the compositional gradient across the boundary.

These two mechanisms of initiation of the discontinuous reaction have been experimentally observed in more than one alloy system.

1.4 GROWTH OF PRECIPITATES

The most common assumptions used in theories and mechanisms of growth of discontinuous cells are those of an approximately planar front and a constant interlamellar spacing. In reality, however, it is far more usual to find the reaction front being anythig but planar. The interlamellar spacing varies about some

average value but remains constant at any aging temperature.

The only mechanism to account for growth in one direction from a grain boundary is that due to Fournelle and Clark (18) who assumed that grain boundary migration was the dominant factor governing development of the reaction cells. It was also suggested that growth in one direction should take place in a temperature range over which thermally activated boundary migration can occur, in order to minimize the non-equilibrium boundary configuration. In the literature, many systems exhibiting unidirectional cell migration were aged at temperataures higher than half the solidus temperatures in K of the respective alloys. In pucker nucleation mechanism, the growth can occur in both the directions normal to the boundary depending on the initial grain boundary precipitation which can occur on either side of the boundary.

As mentioned earlier, the advancing cell front often has a large curvature and as the reaction proceeds the volume fraction of the transformed region increases and so does the total length of the cell boundary. The lamellae, therefore, must multiply for the interlamellar spacing characteristic of the isothermal transformation temperature of the alloy to be maintained. Photomicrographs by Gupta (19) clearly show lamellae multiplication by branching. The multiplication of lamellae may also occur due to repeated nucleation of the precipitate at the migrating cell front, and in cell boundary recess as theoretically predicted by Sundquist (20). Gupta (19) reports that an approximately constant interlamellar spacing was maintained when the cell boundary was moving convexly forward, whereas the value

of the spacing was more than the average in cases when the cell front was moving concavely forward.

1.5 DRIVING FORCE FOR INITIATION OF REACTION

Discontinuous precipitation of $M_{23}C_6$ in austenitic stainless steel has been studied by Hillert and Lagneborg (21), specifically in an attempt to identify the initiation forces. The possible forces considered were: (a) ΔG_{GB} or ΔG_{def} if grain growth or recrystallization were favoured in the absence of precipitation; (b) ΔG_{ppt}, if , following precipitation, interfcial energy considerations favour replacive boundary motion; (c) ΔG_{ε} if precipitation causes steep compositional gradients; and (d) chemical free energy change ΔG_c. The observation of grain boundary bulging in regions devoid of precipitates indicated the potency of (a) and suggested that (b) was not an essential element of initiation. Mechanism (d) was identified as providing the driving force for boundary migration once an element of the boundary had started to move. In summary, the proposed driving forces to initiate the discontinuous reaction ΔG_1 may be written as

$$\Delta G_1 = \Delta G_{ppt} + \Delta G_{GB} + \Delta G_{def} + \Delta G_{\varepsilon} \qquad (1.5)$$

where any combination of one or more of the components may act in a particular alloy system.

1.6 KINETICS OF DISCONTINUOUS PRECIPITATION - THEORETICAL MODELS

Several well developed theories have attempted to explain the growth kinetics of discontinuous precipitation. In his model, Zener (22) uses the morphological similarity between eutectoid and

discontinuous reactions to assume that all the available free energy for the transformation goes to create α/ε interfaces with a critical spacing S. He assumed volume diffusion control in his model and derived an expression for the growth rate ν:

$$\nu = \frac{K_1 D_V}{S} \tag{1.6}$$

where D_V is the volume diffusion coefficient and K_1 is a constant proportional to the concentration difference across the advancing interface.

However, three is scant experimental support for volume diffusion control of the reaction.

1.6.1 Turnbull's Model for Growth

Assuming lamellar morphology of the product phase, Fick's first law may be used to estimate the total solute flow away from a lamellar as

$$\frac{dm}{dt} = \frac{AD}{V_m}\frac{dX_B}{dx} = \frac{AD}{V_m}\frac{\Delta X_B}{L_{eff}} \tag{1.7}$$

where A = Area through which the flux is considered

D = Diffusivity of solute

$\frac{\Delta X_B}{L_{eff}}$ = Concentration gradient of solute

V_m = Molar volume of the α phase

Turnbull's (23) model is based on diffusion of solute through the grain boundary. Assuming a section of vertical length b, A may be substituted by $b.\delta$, where δ is the grain boundary thickness. The diffusion direction is from the α to the ε phase and L_{eff}, therefore, may be taken as S^{α}, the spacing of the α

lamella. This yields

$$\frac{dm}{dt} = \frac{b.\delta.D_b}{V_m} \cdot \frac{\Delta X_B}{S^{\alpha}} \qquad (1.8)$$

Using Lever rule, the width of the lamellae may written as

$$\frac{S^{\alpha}}{V_m} = \frac{X_B^{\varepsilon} - {}^1X_B^{\alpha}}{X_B^{\varepsilon} - X_B^{\alpha}} \frac{S}{V_m}; \quad \frac{S^{\varepsilon}}{V_m} = \frac{{}^1X_B^{\alpha} - X_B^{\alpha}}{X_B^{\varepsilon} - X_B^{\alpha}} \frac{S}{V_m} \qquad (1.9)$$

which gives

$$\frac{dm}{dt} = \nu b \frac{S^{\alpha}}{V_m} \left[{}^1X_B^{\alpha} - X_B^{\alpha} \right] = \nu b \frac{S^{\varepsilon}}{V_m} \left[X_B^{\varepsilon} - {}^1X_B^{\alpha} \right]$$

$$\nu b \frac{S}{V_m} f^{\alpha} f^{\varepsilon} \left[X_B^{\varepsilon} - X_B^{\alpha} \right] \qquad (1.10)$$

Equating (1.8) and (1.10) we get

$$\nu = \frac{D_b \delta}{({}^1X_B^{\alpha} - X_B^{\alpha})} \frac{\Delta X_B}{(S^{\alpha})^2} \qquad (1.11)$$

Turnbull neglects the effects of surface energy and approximated ΔX_B as $({}^1X_B^{\alpha} - X_B^{\alpha/\varepsilon})$. He also neglected X_B^{α} in comparison to ${}^1X_B^{\alpha}$, the original alloy composition. Therefore,

$$\nu = \frac{D_b \delta}{(S^{\alpha})^2} \frac{{}^1X_B^{\alpha} - X_B^{\alpha/\varepsilon}}{{}^1X_B^{\alpha}} \qquad (1.12)$$

1.6.2 Cahn's Model

Cahn (24) in his model took into account the experimentally established fact that the depleted α in equilibrium with ε is not of equilibrium composition and that due to incomplete segregation

of solute only a fraction of the total free energy available is used to drive the reaction, the rest being utilized in forming the interface between depleted α and the precipitate ε. He assumed that the reaction proceeds as far as diffusion would permit and that the interface is flat and no diffusion occurs except at the boundary. Under steady state

$$\frac{\partial X_B^{\alpha}}{\partial t} = \frac{D_b \delta}{V_m} \frac{\partial^{2b} X_B^{\alpha}}{\partial y^2} + \frac{\nu}{V_m} \left({}^{1}X_B^{\alpha} - X_B^{\alpha} \right) = 0 \qquad (1.13)$$

where ν = growth velocity

${}^{b}X_B^{\alpha}$ = solute concentration in the boundary

${}^{1}X_B^{\alpha}$ = original alloy composition

X_B^{α} = depleted α composition

and y = distance along the boundary measured perpendicular to the lamellae.

Assuming the solute concentration in the boundary ${}^{b}X_B^{\alpha} = kX_B^{\alpha}$, where k is the segregation coefficient, and taking the solute

concentration at the three phase intersection to be ${}^{e}X_B^{\alpha}$, we have

$$kD_b \frac{d^2 X_B^{\alpha}}{d(y/s)^2} + \frac{\nu S^2}{\delta} = ({}^{1}X_B^{\alpha} - X_B^{\alpha}) = 0 \qquad (1.14)$$

Solving the above equation and substituting the appropriate boundary conditions

$$({}^{1}X_B^{\alpha} - {}^{e}X_B^{\alpha}) = A \left\{ \text{Cosh} \left[\frac{\nu S^2}{kD_b \delta} \right]^{1/2} \cdot \frac{1}{2} \right\}$$

or

$$A = \frac{({}^{1}X_B^{\alpha} - {}^{e}X_B^{\alpha})}{\text{Cosh } (1/2\ \sqrt{\alpha})} \qquad (1.15)$$

where $\alpha = \dfrac{\nu S^2}{kD_b \delta}$

The fraction of solute transferred through the boundary

$$W = \frac{2}{({}^{1}X_B^{\alpha} - {}^{e}X_B^{\alpha})} \int_0^{1/2} ({}^{1}X_B^{\alpha} - X_B^{\alpha})\, d(y/S)$$

$$W = \frac{2}{\sqrt{\alpha}} \tanh \left(\frac{\sqrt{\alpha}}{2}\right) = \frac{({}^{1}X_B^{\alpha} - X_B^{\alpha})}{({}^{1}X_B^{\alpha} - {}^{e}X_B^{\alpha})} \qquad (1.16)$$

Determining W and hence α gives us a value for $kD_b\delta$ which may be thought of as a combined boundary diffusivity of the solute.

1.6.3 Sundquist's Analysis

Sundquist (20) derived the diffusion equation for the solute transfer through the boundary on the lines of Cahn but instead of assuming a flat interface between α^s and ε phase, he solved the equation for a curved interface. The basic solution of the

diffusion equation gives

$$\frac{(X_B^{\alpha}(\bar{Z}) - {}^{1}X_B^{\alpha})}{X_B^{\alpha/\varepsilon}(0) - {}^{1}X_B^{\alpha})} = \frac{\text{Cosh } (\gamma a - (1 - \bar{Z}))}{\text{Cosh } \gamma a}$$

where

$$a = \frac{\nu S^2}{4\ D_b\ \delta\ k(\overline{\text{Cos } \theta})} \qquad (1.17)$$

$X_B(\bar{Z})$ is the average composition of the depleted matrix at position $(\bar{Z})$ from the interface α and ε phase. $X_B^{\alpha/\varepsilon}(0)$ is the interface composition at the three phase junction. Its value is close to the equilibrium solvus composition at the aging temperataure but is defined by Sundquist (20) as

$$X_B^{\alpha/\varepsilon}(0) = {}^{e}X_B^{\alpha/\varepsilon} \exp \frac{2V_m \theta_o (X_B^{\varepsilon} - X_B^{\alpha})}{RTS^{\alpha}W({}^{1}X_B^{\alpha} - {}^{e}X_B^{\alpha/\varepsilon})} \qquad (1.18)$$

where θ_o has a value of $\pi/6$; $\overline{\text{Cos } \theta}$, which is the average of the cosine of the angle that the normal to the growth front makes with the growth direction, is taken to be 0.7 as proposed by Sundquist.

The parameter 'a' is determined from the relation

$$W = \frac{{}^{1}X_B^{\alpha} \quad X_B^{\alpha/\varepsilon}(0)}{{}^{1}X_B^{\alpha} - {}^{e}X_B^{\alpha/\varepsilon}} \frac{\tanh \gamma a}{\gamma a} \qquad (1.19)$$

1.6.4 Hillert's Analysis

Hillert (25) pointed out that Cahn's (24) treatment of discontinuous precipitation was based on the incorrect assumption that the composition of matrix grain at the line of contact with

precipitate ε, at the growing cell front is equal to the equilibrium value ${}^{e}\chi_B^{\alpha}$. Considering driving forces for α and ε phases separately and assuming that ε phase has constant composition, Hillert (25) obtained an expression for the α/ε interface,

$$\frac{{}^{b}\chi_B^{\alpha} \quad {}^{o}\chi_B^{\alpha}}{{}^{1}\chi_B^{\alpha} - \chi_B^{\alpha}} = \frac{\nu (S^{\varepsilon})^2}{8 D_b \delta} \left\{ 1 - (2y/S^{\varepsilon})^2 \right\} \qquad (1.20)$$

Applying the boundary diffusion control of Turnbull (23)

$$\frac{dm}{dt} = \frac{8\ D_b \delta\ k\ \Delta X}{V_m S}$$

to yield

$$\nu = \frac{8k\ D_b \delta}{S S^{\alpha}} \frac{(\chi_B^{\alpha} - {}^{o}\chi_B^{\alpha})}{({}^{1}\chi_B^{\alpha} - \chi_B^{\alpha})} \qquad (1.21)$$

The two composition terms ${}^{o}\chi_B^{\alpha}$ and χ_B^{α} are treated as constants although they are not true constant compositions. Hillert (25) has given explicit parameters thus enabling the diffusivity $kD_b\delta$ to be evaluated from experimentally measured quantities.

1.6.5 Petermann and Hornbogen Model

According to Petermann and Hornbogen (26), the growth velocity is given by

$$\nu = - M \Delta G \qquad (1.22)$$

where M = grain boundary mobility

ΔG = driving force for growth of cells.

The mobility is a function of temperature and is determined by atomic jump frequency τ^{-1} and grain boundary thickness δ. For

the phase to grow and therefore for continued migration of the grain boundary, solute atoms acquired by the grain boundary must diffuse a distance S/2 to the ϵ lamellae. The time for atoms to move a distance S/2 is

$$\frac{S^2}{4} = 2\, D_b \tau \text{ which gives } \tau = \frac{S^2}{8D_b}$$

The growth rate is related to the diffusivity and interlamellar spacing by the following relation.

$$\nu = - \frac{8D_b \delta}{RTS^2} \Delta G. \qquad (1.23)$$

The amount of chemical free energy available to drive the reaction can be estimated with the help of free energy composition diagram

$$\Delta G = p\ \Delta\ G_c + \frac{2\gamma V_m}{S} \qquad (1.24)$$

where γ = specific surface energy of the α/ϵ interface

p = fraction of chemical free energy ΔG_c released during the reaction.

Using dilute solution model,

$$\Delta G = RT \left[{}^1x_B^\alpha \ln \frac{x_B^\alpha}{{}^1x_B^\alpha} + {}^1x_A^\alpha \ln \frac{x_A^\alpha}{{}^1x_A^\alpha} \right] + \frac{2\gamma V_m}{S} \qquad (1.25)$$

The equation for growth velocity is given by

$$\nu = - \frac{8D_b \delta}{S^2 RT} \left\{ RT \left[{}^1x_B^\alpha \ln \frac{x_B^\alpha}{{}^1x_B^\alpha} + {}^1x_A^\alpha \ln \frac{x_A^\alpha}{{}^1x_A^\alpha} \right] + \frac{2\gamma V_m}{S} \right\} \qquad (1.26)$$

1.7 THE COPPER - ANTIMONY SYSTEM

The equilibrium diagram of the binary Cu-Sb system pertaining to the composition used in this work is given in Fig. (3.4).

A maximum of 6 at. pct. Sb dissolves in Cu at 918^{o}K. The aging was done in a temperature range in the two phase $\alpha+\varepsilon$ region. The dissolution temperature ranged from 730 K to a little below the equilibrium solvus temperature (650K).

The ε phase is a superstructure of h.c.p. type. The reported lattice parameters are a= 10.836$\mathring{A}$, c = 8.611 $\mathring{A}$, and c/a = 0.7947. A unit cell of the ε phase contains 54 atoms.

CHAPTER 2

EXPERIMENTAL PROCEDURE

2.1 Alloy Preparation

The alloy for this work was prepared by melting required amounts of copper and antimony together in a sealed quartz tube under vacuum. Cylindrical rods of the alloy (8mm dia) were sealed in quartz tube under vacuum and homogenized at 650^{o}C for 12 days. The alloy was aged at 327^{o}C for 200h followed by homogenization at 550^{o}C for an hour and subsequently aged at 327^{o}C for 200h. A final anneal of 3h at 550^{o}C was given. This thermal cycling helped in breaking the cast structure and in producing a polycrystalline grain structure.

The alloy thus prepared was cut into thin discs of 1 mm thickness with a diamond cutter.

2.2 Heat Treatment

In order to study the kinetics of discontinuous precipitation the alloy specimens were first solution treated for 10 min at 550^{o}C and then isothermally aged in the temperature range 520K to 630K for different times. Solutionizing and aging was done in a salt bath comprising 50% $NaNO_2$ and 50% KNO_3. The aging temperatures were maintained withi a range of ± 2^{o}C. Ice cold water was used for quenching.

The heat treated samples were cold mounted using powder resin and liquid hardener. The oxidized surface layers were removed by grinding. These were then polished and etched for metallographic examination. $FeCl_3$ solution was used as the etchant.

2.3 Optical Microscopy

The growth distance at each time was measured as the perpendicular distance between the original grain boundary position and the cell front. About 40 measurements were made for each specimen and the growth distance values were averaged. These average values were further multiplied by $\pi/4$ to be consistent with the bulk averaging technique used by Gust et al (27).

Optical microscopy was also used to determine the average interlamellar spacing in samples aged at 630K, 615K, 600K and 580K. Again about 50 measurements were made to find out the average interlamellar spacing at each temperature.

The interlamellar spacing for the rest of the samples were determined from photomicrographs obtained using scanning electron microscope.

2.4 X-Ray Analysis

The composition of the depleted α matrix was determined by X-ray diffraction using Cu-K_α radiation with Ni filter. The 2θ values corresponding to {311} peak position were determined at a scanning speed of $0.3^{o}min^{-1}$. The data were corrected for instrumental error by taking the 2θ value of the {311} peak for a high purity copper sample. The lattice parameters corresponding to each peak were determined and the depleted α composition found from the composition - lattice parameter data reported by Mertz et al (40).

CHAPTER 3

RESULTS AND DISCUSSION

3.1 MORPHOLOGY OF DISCONTINUOUS REACTION PRODUCTS

It was observed that the reaction started at the grain boundaries. The products, in lamellar form, formed cells which grew with the boundary migrating forward and sweeping the supersaturated α region with time. Boundaries with cells on one side as well as those with cells on both sides were observed and it may be inferred that the same boundary may have opposite tilts which may be responsible for such an observation. At earlier stages of the transformation, there were some boundaries with no cells. This proves the fact that the reaction initiation is sensitive to the boundary structure and hence energy.

The initiation of precipitation occurs late on low angle boundaries or those with CSL orientation. However, once these boundaries are deflected, there is a continuous change in their orientation to a high energy configuration and hence the boundary mobility increases. The cells maintained more or less uniform interlamellar spacing, as may be observed in Figure 3.1(a,b).

3.2 GROWTH RATE

For each aging temperature the growth distance of the grain boundary precipitate corresponding to each time of transformation was measured using optical microscopy. About 40 measurements were made from each specimen and the distance values were multiplied by $\pi/4$ to be consistent with the bulk averaging technique used by

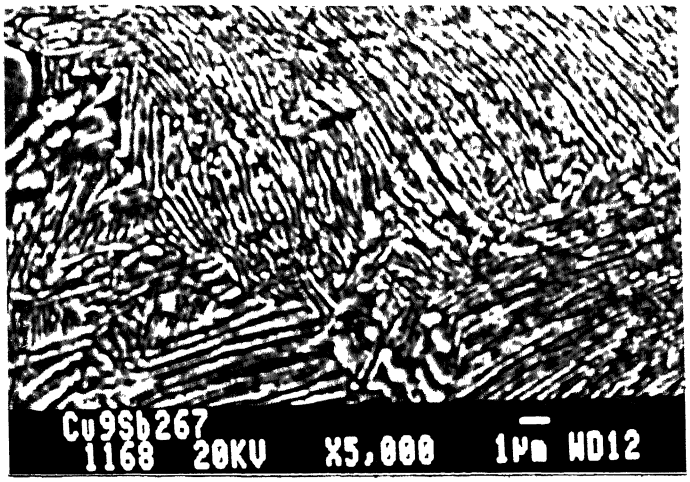

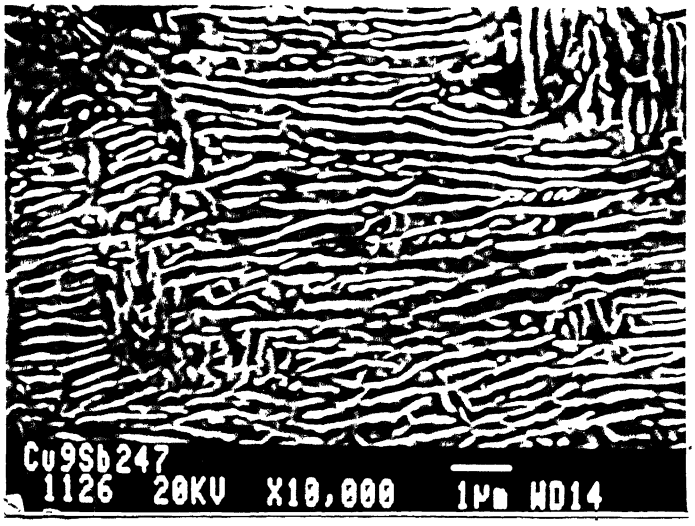

1. Fig. 3.1a,b Photomicrographs showing the lamellar structure of the cellular product.

Gust et.al.(27). This was done so as to average all orientations of cells originating from grain boundaries of different misorientation. The growth distance data was plotted against time for each temperature and the growth rate was estimated from the gradient of the linear plot.

The growth rate vs. temperature plot is shown in Figure 3.2. From the figure it is evident that the double derivative of growth rate with respect to temperature is negative, meaning, the growth rate increases at a decreasing rate. The maximum growth rate of about $3.5 \times 10^{-10} ms^{-1}$ corresponds to 621K. The data matches with that of Gupta and Balasubrahmanyam (28). It also compaires very well with that of Gust and Priedel who measured the growth rate for Cu-5Sb alloy (29) during discontinuous precipitation. Gust and Priedel (29) obtained a maximum value of about $4 \times 10^{-10} ms^{-1}$ at 620K. The higher value is expected since the Sb concentration of their alloy was slightly higher than that used in this investigation.

3.3 INTERLAMELLAR SPACING

Table 3.1 presents the interlamellar spacing data for the primary cells at various temperatures of transformation. Each data is an average of about 50 measurements made randomly on the fully transformed specimen, multiplied by π /4 for the same reason as stated before. The data is plotted against temperature in Figure 3.3. The interlamellar spacing decreases continuously with decreasing aging temperature as expected. Though the cell growth rate is lower at lower temperatures, this observation is due to the decrease in the diffusion distance of the solute because of

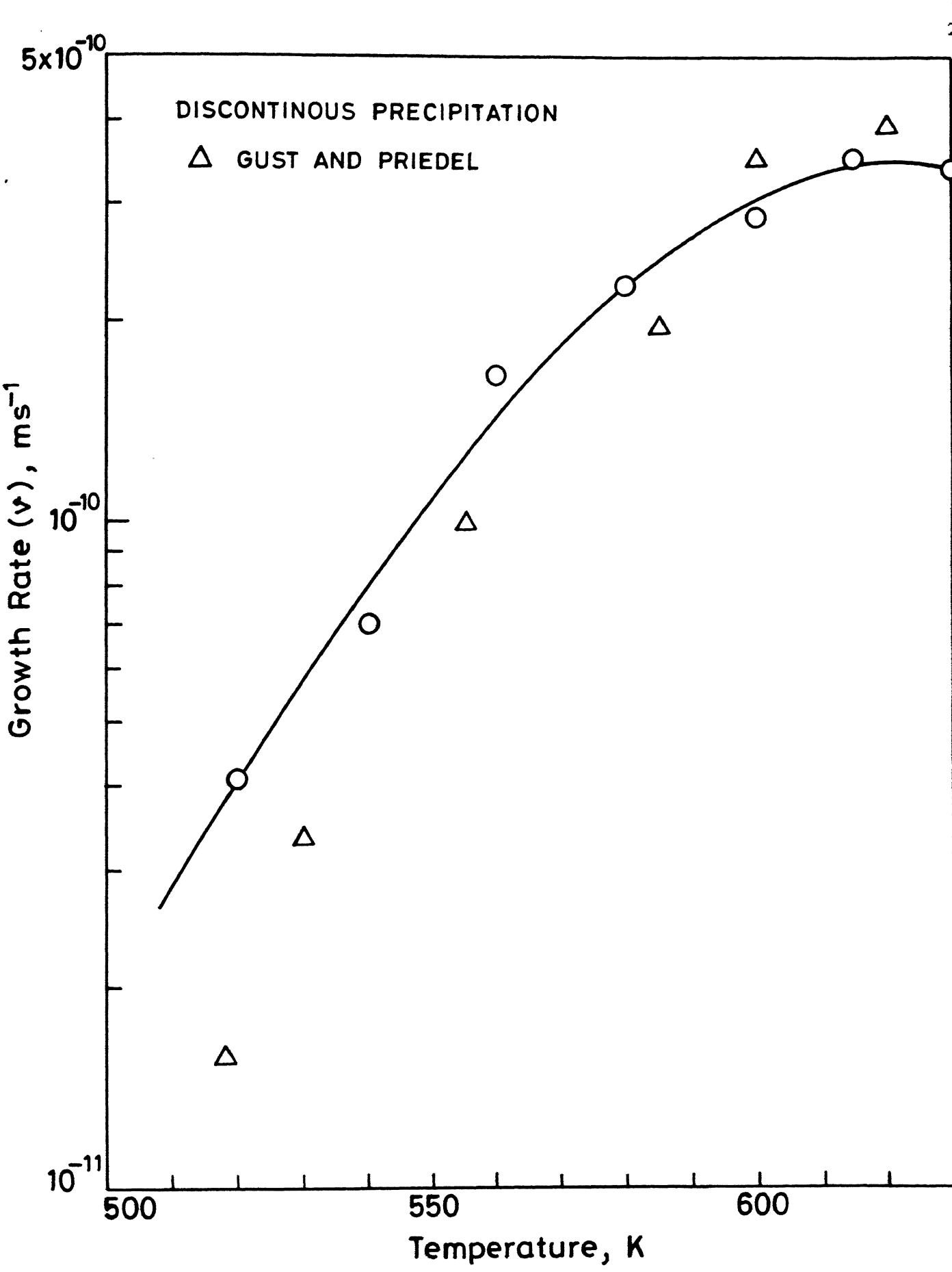

2. Fig. 3.2 Plot of rate of growth of discontinuous cells vs. temperature.

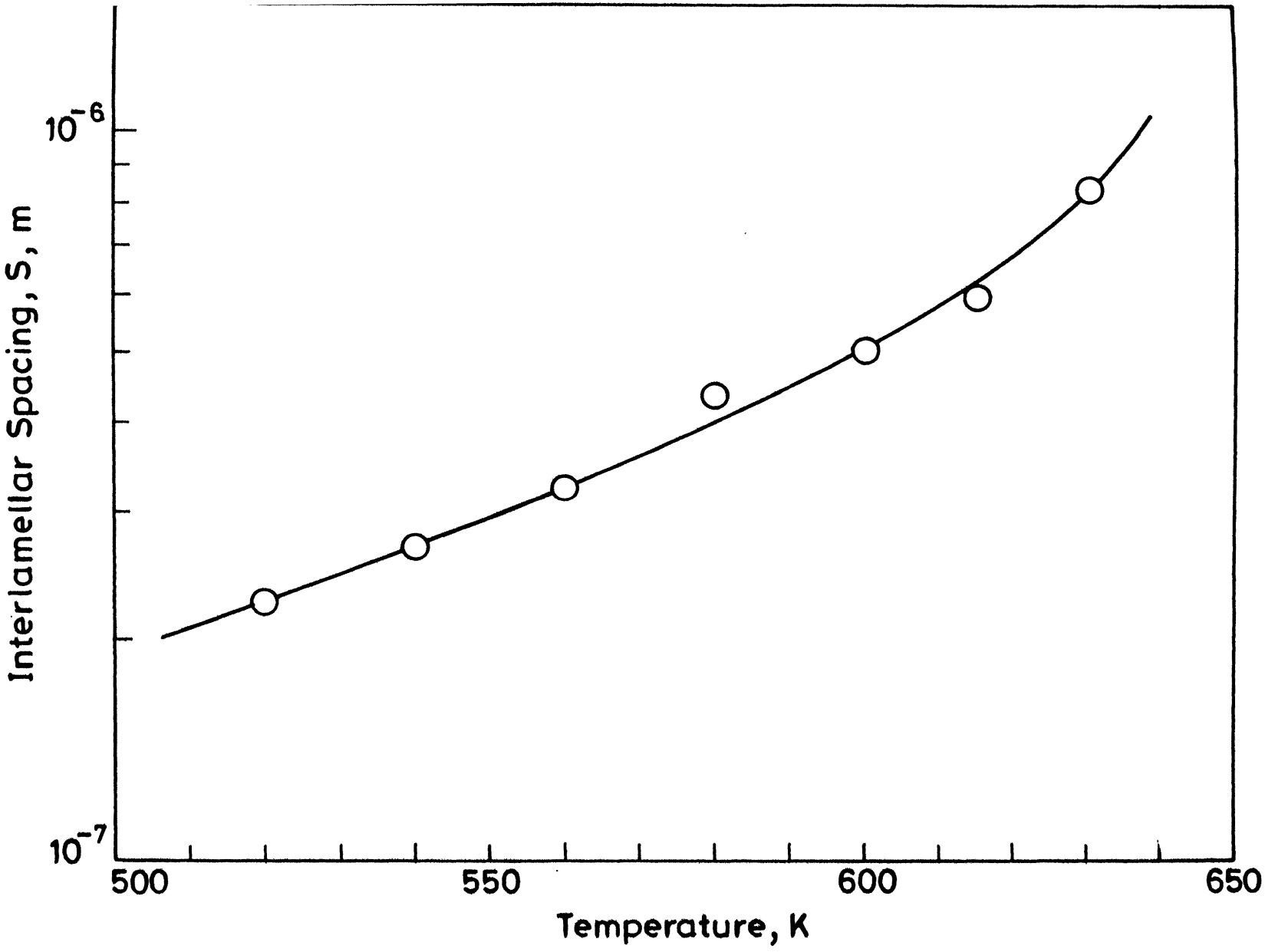

3. Fig. 3.3 Plot of interlamellar spacing vs. temperature.

TABLE 3.1

T(K)	$^{p}x_{B}^{\alpha}$	$^{e}x_{B}^{\alpha}$	S_1 (m) ($\times 10^{-7}$)	ν_1 ($\times 10^{-11}$ ms^{-1})
630	0.0364	0.0330	8.42	34.0
615	0.0322	0.0292	6.00	35.3
600	0.0285	0.0260	5.10	28.8
580	0.0251	0.0220	4.41	22.7
560	0.0212	0.0185	3.25	16.7
540	0.0178	0.0156	2.70	7.03
520	0.0170	0.0128	2.24	4.08

TABLE 3.2

T(K)	L	ΔG_1^c	ΔG_1^γ	ΔG_1	$kD_b\delta$ $(m^3 s^{-1})$
630	3.6821	-14.216	7.06	-7.1471	2.208 x 1
615	3.7467	-23.048	9.92	-13.13	6.185 x 1
600	3.8095	-32.732	11.67	-21.06	2.21 x 10
580	3.9060	-47.925	13.496	-34.43	7.72 x 10
560	4.0111	-65.875	18.31	-47.56	2.15 x 10
540	4.1169	-84.588	22.04	-62.545	4.59 x 10
520	4.2479	-105.769	26.57	-79.198	1.396 x 1

the lower value of diffusivity at low aging temperatures.

3.4 COMPOSITION OF THE DEPLETED MATRIX

The composition of the depleted matrix is slightly higher than that dictated by the equilibrium solvus. The transformation is accompanied by a lowering of the total free energy of the system. However, a small part of the free energy is retained by the interface between the lamellae. In this sense the transformation remains incomplete in the time allowed for its occurence.

The average compositions of the depleted α matrix, ${}^{p}X_{B}^{\alpha}$, were determined from lattice parameter measurements using X-ray diffraction, and are shown in Table 3.1. The composition of the depleted matrix in equilibrium with the second phase, ε, is shown in Fig. 3.4 along with the equilibrium solvus of the Cu-rich side of the Cu-Sb phase diagram.

3.5 PRIMARY CELL GROWTH KINETICS

In most of the theories that have been proposed to describe the kinetics of cellular phase transformation in substitutional alloys, the growth rate is related to the boundary diffusivity and the interlamellar spacing by the following equation

$$\nu_1 = \alpha' \frac{kD_b\delta}{S_1^2} \qquad (3.1)$$

where α' is related to the composition of the depleted matrix and has different value for various models.

The value of α' for Petermann and Hornbogen (26) theory is

$$\alpha' = -\frac{8\Delta G_1}{RT} \qquad (3.2)$$

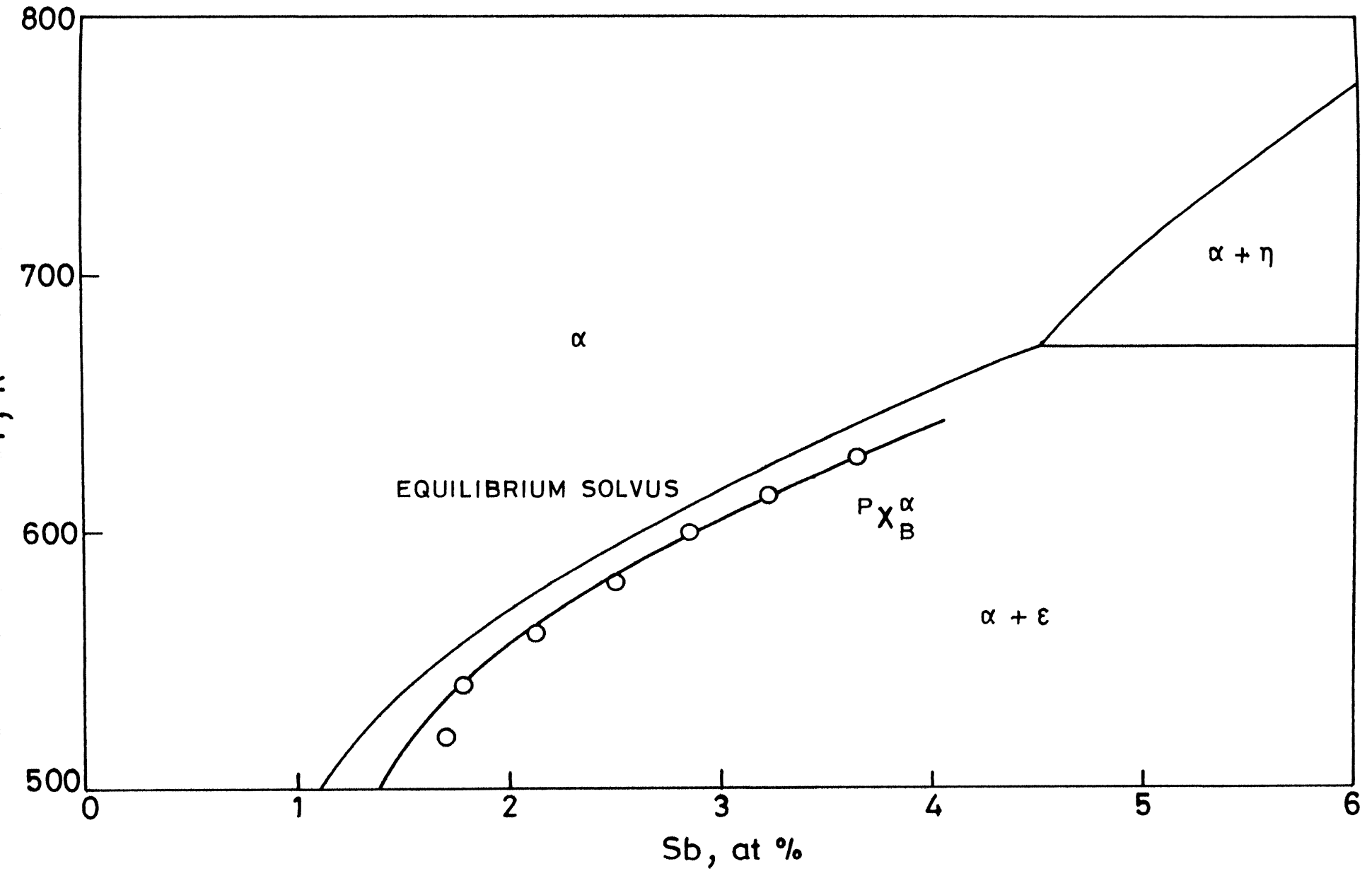

4. Fig. 3.4 Composition of the depleted matrix in equilibrium with the second phase, ε, along

where ΔG_1 is the driving force used for primary cell growth and R, T have their usual meaning. ΔG_1 was determined using

$$\Delta G_1 = \Delta G_1^C + \Delta G_1^\gamma \left(= \frac{2\gamma V_m}{S_1} \right) \qquad (3.3)$$

where ΔG_1^C is the chemical free energy available for the discontinuous reaction and γ is the interfacial energy of the α/ε interface. In Cu-Sb system, an increase in grain boundary energy from 280 to 320 mJm^{-2} has been reported to result due to increase in Sb content from 0.57 to 0.78 at.% (30). Taking the temperature coefficient of the grain boundary energy for Cu and Cu-base systems to be $-0.1\ mJm^{-2}K^{-1}$ (30), the grain boundary energy is estimated to be around 400 mJm^{-2} in the range of aging temperatures used in this investigation.

Using the regular solution model,

$$\Delta G^\alpha = RT \left[X_A \ln X_A + X_B \ln X_B \right] + LRT\, X_A^\alpha\, X_B^\alpha \qquad (3.4)$$

The value of the free energy of formation, ΔG^ε, when used in the equation outlined by Chuang et. al (31) gives the value of L as

$$L = \frac{\frac{\Delta G^\varepsilon}{RT} - \left[X_B^\varepsilon \ln {}^eX_B^\alpha + (1 - X_B^\varepsilon) \ln (1 - {}^eX_B^\alpha) \right]}{\left[({}^eX_B^\alpha)^2 + X_B^\varepsilon\, (1 - 2\,{}^eX_B^\alpha) \right]} \qquad (3.5)$$

where X_B^ε is the composition of the ε phase (=0.19) and ${}^eX_B^\alpha$ is the equlibrium solvus composition of α at the aging temperature. Using the value of L (Table 3.2) thus obtained, the free energy of the $(\alpha+\varepsilon)$ phase mixture, $\Delta G_1^{\alpha+\varepsilon}$, has been obtained at each

temperature at the original alloy composition using

$$\Delta G_1^{\alpha+\varepsilon} = \left[\frac{X_B^{\varepsilon} - {}^1X_B^{\alpha}}{X_B^{\varepsilon} - {}^pX_B^{\alpha}}\right] \Delta G_1^{\alpha} + \left[\frac{{}^1X_B^{\alpha} - {}^pX_B^{\alpha}}{X_B^{\varepsilon} - {}^pX_B^{\alpha}}\right] \Delta G^{\varepsilon} \qquad (3.6)$$

where ΔG_1^{α} is the value of ΔG^{α} at the composition of the depleted matrix.

The chemical free energy of the primary cellular reaction is given by

$$\Delta G_1^{c} = \Delta G_1^{\alpha+\varepsilon} - \Delta G_o^{\alpha} \qquad (3.7)$$

where ΔG_o^{α} is the value of ΔG^{α} at the original alloy composition. The chemical free energy data are given in Table 3.2.

Dilute solution model was also used to determine ΔG_1^{c} according to the equation

$$\Delta G_1^{c} = RT \left[{}^1X_B^{\alpha} \ln \frac{{}^pX_B^{\alpha}}{{}^1X_B^{\alpha}} + (1 - {}^1X_B^{\alpha}) \ln \frac{(1 - {}^pX_B^{\alpha})}{(1 - {}^1X_B^{\alpha})}\right] \qquad (3.8)$$

According to the model of Hillert (25), the value of the parameter α' is given by

$$\alpha' = \frac{BS_1}{S_1^{\alpha}} \left[\frac{X_B^{\alpha} - X_B^{\alpha/\varepsilon}}{{}^1X_B^{\alpha} - X_B^{\alpha}}\right] \qquad (3.9)$$

where X_B^{α} is the variable composition of the α phase and $X_B^{\alpha/\varepsilon}$ is the interface composition. Taking $L^{\alpha} = L^{\varepsilon} = 0.5$ and $K^{\alpha}=1$ as suggested by Hillert (25), the modified α' is

$$\alpha' = \frac{4S_1}{S_1^{\alpha}} \tag{3.10}$$

Avoiding the above simplification, since the values of L^{α}, L^{ε} and K^{α} are not known, substitution of $X_B^{\alpha/\varepsilon} = {}^{e}X_B^{\alpha}$ and $X_B^{\alpha} = {}^{p}X_B^{\alpha}$ yields a modified value for α' given by

$$\alpha' = \frac{8S_1}{S_1^{\alpha}} \left[\frac{{}^{p}X_B^{\alpha} - {}^{e}X_B^{\alpha}}{{}^{1}X_B^{\alpha} - {}^{p}X_B^{\alpha}} \right] \tag{3.11}$$

The value of α' in equation (3.1) for the theory of cellular precipitation after Cahn (24) is

$$\alpha' = 4\eta \tag{3.12}$$

where η is related to the fraction of the supersaturation recovered, W, by the following relation

$$W = \frac{{}^{1}X_B^{\alpha} - {}^{p}X_B^{\alpha}}{{}^{1}X_B^{\alpha} - {}^{e}X_B^{\alpha}} = \frac{\tanh \sqrt{\eta}}{\sqrt{\eta}} \tag{3.13}$$

The model of Turnbull (23) for the kinetics of the discontinuous reaction gives the value of the parameter α' as

$$\alpha' = \frac{{}^{1}X_B^{\alpha} - {}^{e}X_B^{\alpha}}{{}^{1}X_B^{\alpha}} \tag{3.14}$$

TABLE 3.3

T(K)	ΔG_1^c	ΔG_1	$kD_b\delta$ $(m^3 s^{-1})$
630	-10.72	-3.66	4.31×10^{-20}
615	-20.04	-10.12	8.02×10^{-21}
600	-31.286	-19.61	2.38×10^{-21}
580	-44.24	-30.744	8.65×10^{-22}
560	-63.56	-45.25	2.26×10^{-22}
540	-84.94	-62.9	4.57×10^{-23}
520	-88.188	-61.62	1.79×10^{-23}

TABLE 3.4

$kD_b\delta$ (m^3s^{-1})

T(K)	Cahn	Turnbull	Hillert
630	7.04×10^{-23}	7.38×10^{-22}	2.18×10^{-23}
615	5.72×10^{-23}	3.14×10^{-22}	1.205×10^{-23}
600	5×10^{-23}	1.59×10^{-22}	7.28×10^{-24}
580	2.78×10^{-23}	8.0×10^{-23}	4.17×10^{-24}
560	1.48×10^{-23}	2.83×10^{-23}	1.678×10^{-24}
540	6.0×10^{-24}	7.5×10^{-24}	4.899×10^{-25}
520	1.26×10^{-24}	2.77×10^{-24}	1.86×10^{-25}

The values of the various free energies at different aging temperatures and the corresponding boundary diffusivities are presented in Table 3.2 for regular solution model, and in Table 3.3 for dilute solution model.

From experimentally determined values of growth rate, interlamellar spacing and composition for the alloy, the $kD_b\delta$ values were estimated for each aging temperature for the remaining three models and these are presented in Table 3.4. The temperature dependence of diffusivity is shown in Figure 3.5. The data fall on straight lines for all the four models except for Cahn's model which shows a deviation from linearity at higher temperatures. The activation energies calculated from the slopes of the lines range between 127 and 180 kJ mol^{-1} as shown in Table 3.5.

Table 3.5

Model	Activation Energy, Q
Petermann & Hornbogen	180 $kJmol^{-1}$
Cahn	133 $kJmol^{-1}$
Turnbull	138 $kJmol^{-1}$
Hillert	127 $kJmol^{-1}$

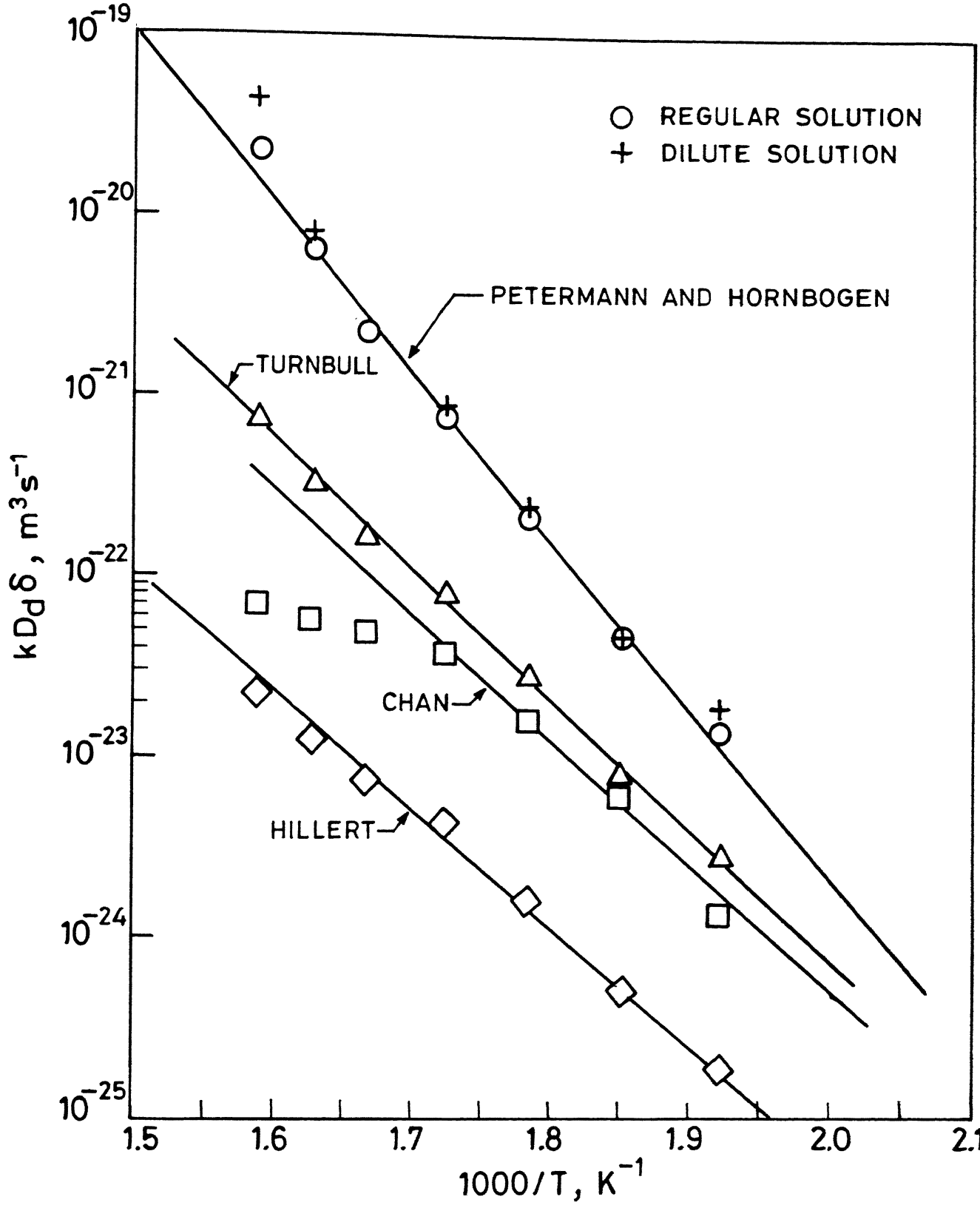

5. Fig. 3.5 Temperature dependence of diffusivity values determined using the models of Petermann and Hornbogen, Cahn, Hillert, and Turnbull.

The models after Cahn, Turnbull, and Hillert give activation energy of about 135 kJ mol^{-1}, which is about two thirds of the activation energy for lattice diffusion of Sb in Cu-Sb system reported to be 200 kJ mol^{-1} (32). However, the model after Petermann and Hornbogen gives an activation energy which is very close to that for tracer diffusion of Sb in Cu reported by Inman et.al (33) to be 176± 3kJmol^{-1}. This value gives the value of volume diffusivity, D_V, at 600K to be about 2 x $10^{-20} m^2 s^{-1}$. Clearly the observed values of the diffusivities are 7 to 8 orders of magnitude higher than this value.

Renouff (34) has measured the grain boundary diffusivity of Sb in Cu in the range of 878 to 994K. The extrapolated diffisivities for this investigation in this given range are two to four orders of magnitude higher than the boundary diffusivities for stationary boundaries.

From the diffusivity values of the discontinuous reaction in the present alloy, it may be concluded that the cellular phase transformation in Cu-9 wt% Sb alloy takes place by the transport of Sb atoms along the migrating grain boundaries.

CHAPTER 4

DISCONTINUOUS DISSOLUTION

4.1 INTRODUCTION

It has been observed that the cellular product of discontinuous precipitation, when taken to a temperature a little above the solvus for the alloy, undergoes a discontinuous mode of dissolution governed by solute transport through the grain boundaries. The discontinuous dissolution of cellular precipitates has been studied in Cu-Cd (35,36), Pb-Sn (37), Al-Zn (38) and Cu-In (39) alloys. The lamellar product of discontinuous precipitation is dissolved at a temperature above the solvus or 20-30K below it. A characteristic feature of all the above studies is that the solidus temperature corresponding to the alloy composition was low enough to limit volume diffusion of solute. The dissolution cells have been observed to initiate at the original position of the grain boundary and at cell boundary intersections. A slab of the dissolved region forms by coalescence of the dissolution cells nucleated at grain boundaries and moves forward with time of dissolution.

Tu and Turnbull (37) have reported that the dissolution of lamellar precipitates is a cellular mode of transformation. The cell boundary acting as a short circuit path of diffusion, recedes, thereby dissolving the precipitates. The orientation of the transformed matrix follows the same relationship as that in cellular precipitation. Their measurement of rate of dissolution (37) are in agreement with a kinetic analysis which assumes a

boundary diffusion controlled process.

The driving force of dissolution which tends to move back the cell boundary may be written as

$$\Delta G_d = \Delta G_d^c - \frac{2\gamma V_m}{S} \qquad (4.1)$$

In the dissolution process, if the dissolution temperature is close to the solvus temperature, the magnitude of the surface term in the above equation will not differ much from the volume term. A larger surface term would make the dissolution experiment more accurate, so it would be worthwhile to have specimens in which cellular precipitation was effected at a low temperature in order to develop a finer lamellar structure (37).

The present investigation has been extended to the study of the kinetics of discontinuous dissolution in the same Cu-Sb alloy so as to estimate the diffusivity values and thereby establish the rate controlling process.

4.2 EXPERIMENTAL PROCEDURE

4.2.1 Starting Specimens

The alloy was prepared on the same lines as outlined in section 2.1. The cut specimens were vacuum sealed in a quartz tube and held at 327 $\pm 2^{o}$C for 240 hrs and then quenched in ice cold water. This resulted in almost 100% transformation into cellular precipitates.

4.2.2 Dissolution Treatment

Dissolution in the transformed samples was carried out in salt bath made of 50% KNO_3 and 50% $NaNO_2$. The treatment was done at temperatures ranging from 650K to 730K at regular intervals of 10K. The treatment time ranged from a few seconds at high temperatures to a few minutes at the lowest temperature. An additional second was allowed to enable the specimens to equilibrate with the bath temperature. The specimens were immediately quenched in ice cold water.

4.2.3 Optical Microscopy

The specimens treated at various temperatures were cold-mounted and polished for optical metallographic examination. The etchant used was $FeCl_3$ solution.

The growth distance of the dissolution cell was measured using optical microscopy by measuring the perpendicular distance between the cell front and the grain boundary from which it had started to grow. More than 40 measurements were made on each specimen and the data was averaged multiplied by $\pi/4$ to be consistent with the bulk averaging technique, as mentioned earlier.

4.3 RESULTS AND DISCUSSION

4.3.1 Morphology of Dissolution Cells

The microstructures after dissolution for 40 s and 50 s at 660K are shown in Figure 4.1(a,b). The figure clearly shows that the dissolution cells formed on one side of the grain boundary as well as on both sides of it. In each case the dissolution occured by migration of the cell boundary. Cells were formed at

(a)

(b)

6. Fig. 4.1a,b Microstructures after dissolution treatment for (a) 40s and (b) 50s at 660K.

prior grain boundaries and at cell boundary intersections. The microstructure during dissolution has many similarities with the structure observed during nucleation and growth of cellular precipitate. Increasing the time of dissolution increased the volume fraction of the dissolution cells.

4.3.2 Growth Rate

The averaged growth distances were plotted against the time of dissolution of each temperatuare. In this case also, the plots are observed to be linear and the slope gave the rate of growth value at each temperature. Figure 4.2 gives the plot of growth rate of dissolution, as a function of temperature.

The growth rates for both precipitation and dissolution are plotted in Figure 4.3. Clearly, from this figure, the dissolution growth rates are about two orders of magnitude higher than those of precipitation.

4.3.3 Kinetics of Discontinuous Dissolution

Following the theory of Petermann and Hornbogen (26) for cellular precipitation, Gupta (39) has shown that the rate of growth of cells during dissolution is related to the diffusivity by the following equation

$$\nu = - \frac{8}{RT} \frac{kD_b \delta}{S^2} \Delta G_d \qquad (4.2)$$

where ΔG_d is the driving force for dissolution, S is the interlamellar spacing, Δ is the width of the grain boundary, k is the segregation ratio and RT have their usual meaning. The

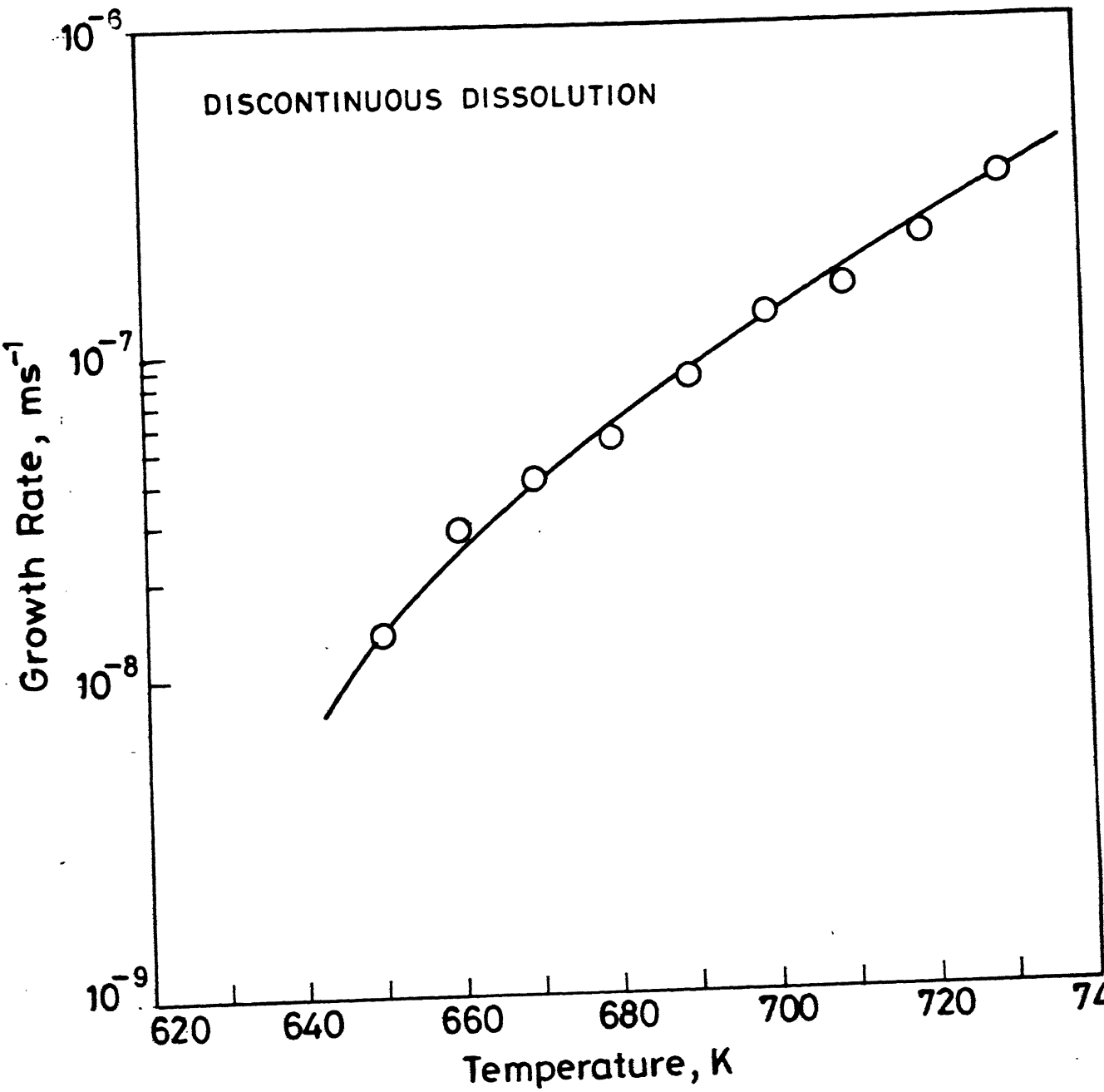

7. Fig. 4.2 Plot of growth rate of dissolution as a function of temperature.

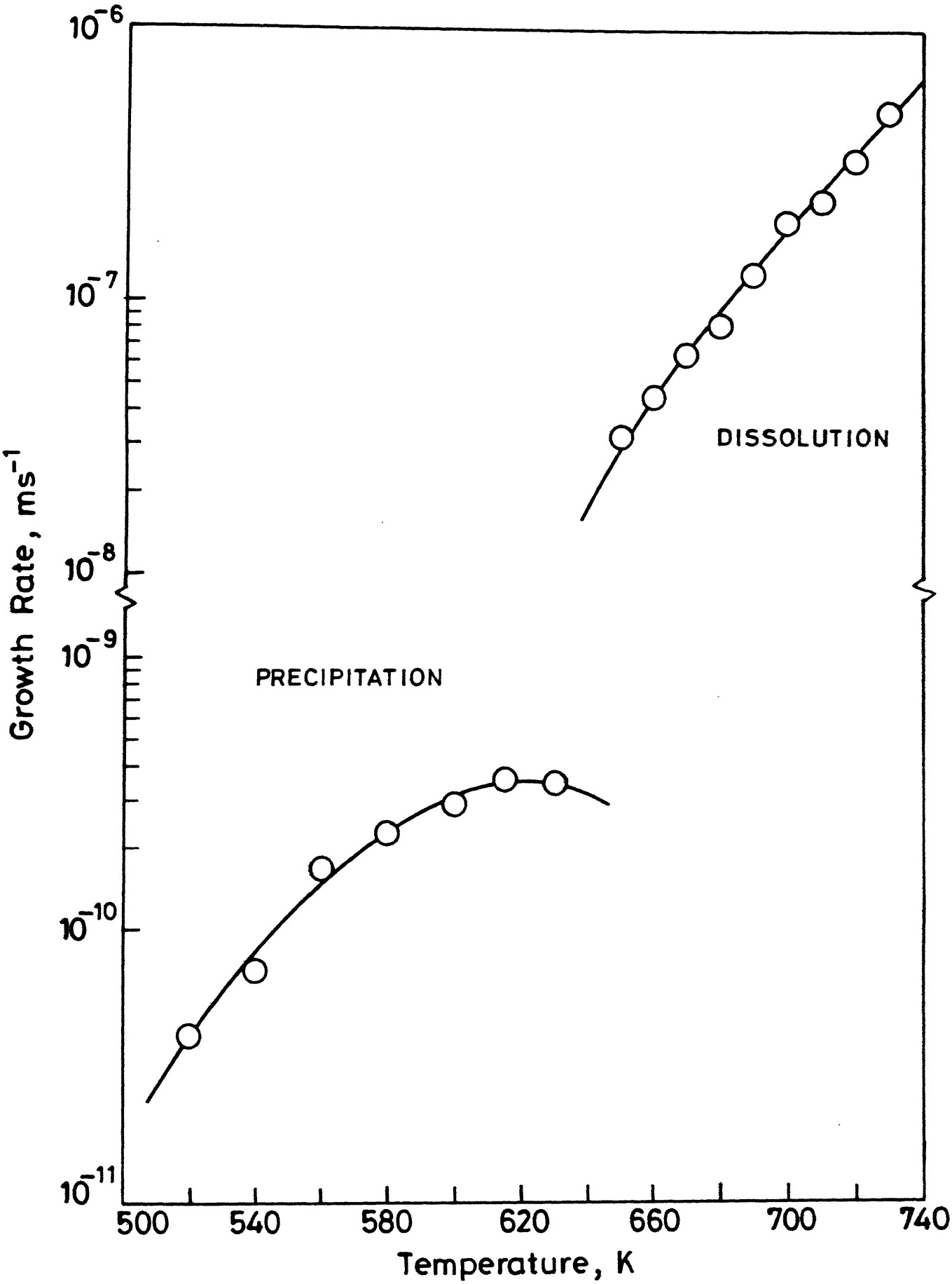

8. Fig. 4.3 Comparative growth rates of precipitation and

driving force for dissolution is obtaiined by adding the surface free energy to the chemical free energy for dissolution ΔG_d^c, since the α/ε interfacial energy is fully recovered during dissolution.

$$-\Delta G_d = \left| \Delta G_d^c \right| + \frac{2\gamma V_m}{S} \qquad (4.3)$$

The chemical free energy for dissolution as obtained by writting the second derivation of the Gibbs free energy as a function of solute concentration, for the regular solution model, is given by:

$$\Delta G_d^c = -\frac{1}{2} RT \left[\frac{1 - 2L\ {}^1X_A^\alpha\ {}^1X_B^\alpha}{{}^1X_A^\alpha\ {}^1X_B^\alpha} \right] (\Delta X_B^\alpha)^2 \qquad (4.4)$$

where ΔX_B^α is the difference in the recovered composition of solute after dissolution and the composition of solute in the depleted α matrix in contact with ε in the original lamellar structure.

Table 4.1 gives the estimated values of ΔG_d, ν, and $kD_b\delta$ values are plotted against temperature on a log-log scale in Figure 4.4. The plot corresponding to the model of Petermann and Hornbogen (26) for cellular precipitation is also drawn in the same figure. The activation energy calculated from the slope of the straight line is 136 kJ mol^{-1}. This value is in good agreement with the value of 140 kJ mol^{-1} determined by Gupta et al (28) for a Cu-5.5Sb alloy. Also, this value matches well with those obtained for cellular precipitation using the models after Cahn (24), Turnbull (23) and Hillert (25). One may infer from this that the processes of disconcontinuous precipitation and

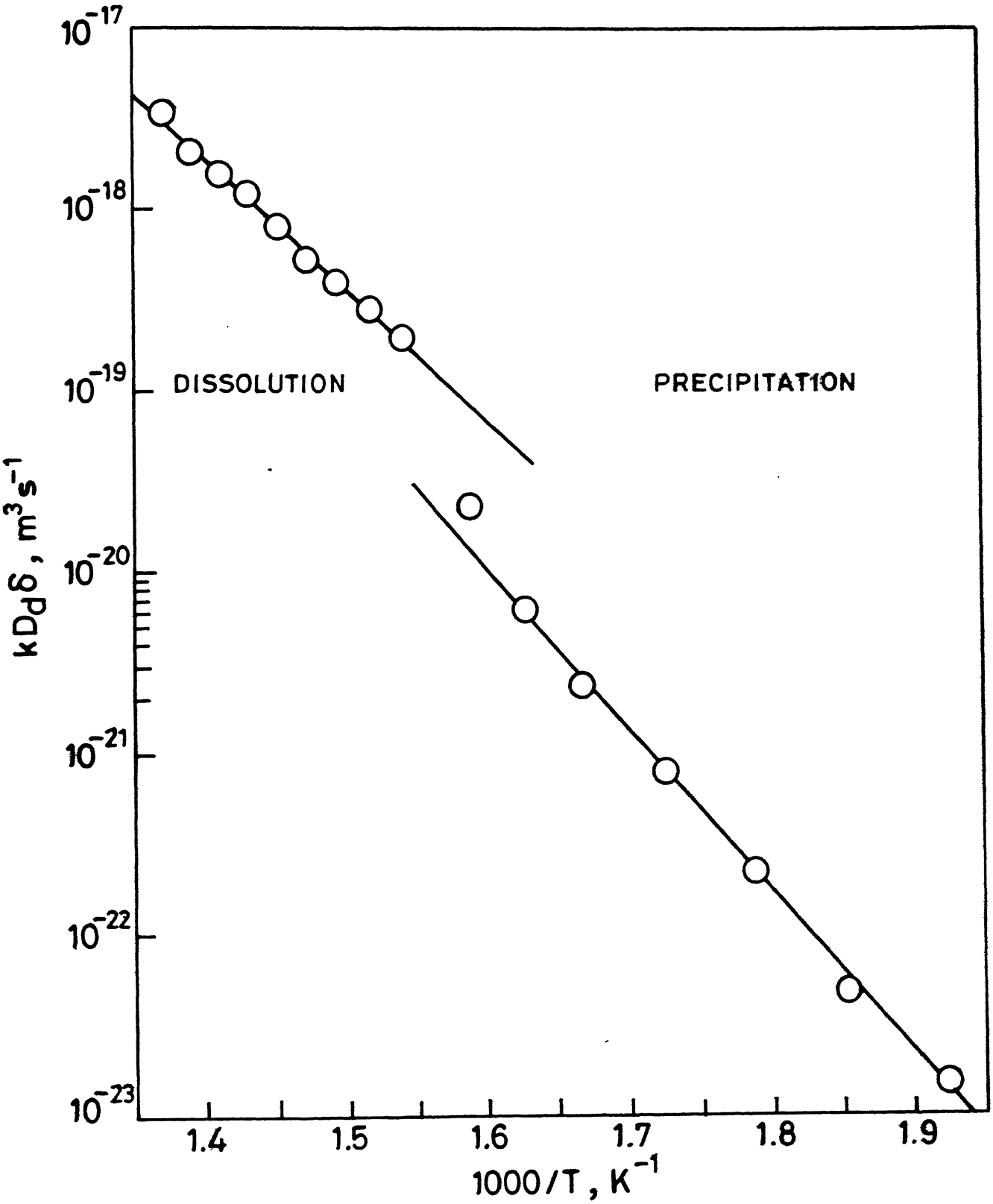

9. Fig. 4.4 Plot of $kD_b\delta$ for dissolution vs. 1/T.

dissolution involve similar mechanism. Also, the $kD_b\delta$ values clearly establish that the dissolution reaction is controlled by the diffusion of Sb along the cell boundaries at the temperatures used for this study.

TABLE 4.1

$^{1}X_{B}^{\alpha} = 0.049$ $\quad S = 5.1\times10^{-7}$ $\quad V_m = 7.4\times10^{-6} m^3 mol^{-1}$

$^{1}X_{A}^{\alpha} = 0.951$ $\quad \gamma = 0.4\ Jm^{-2}$ $\quad \frac{2\gamma V_m}{S} = 11.67\ J\ mol^{-1}$

T(K)	L	ΔG_d ($J\ mol^{-1}$)	ν ($\times10^{-7} ms^{-1}$)	$kD_b\delta$ ($m^3 s^{-1}$)
730	3.4889	-30.138	5.01	3.28×10^{-18}
720	3.4936	-29.874	3.301	2.15×10^{-18}
710	3.4999	-29.60	2.35	1.52×10^{-18}
700	3.5044	-29.34	1.95	1.25×10^{-18}
690	3.5081	-29.08	1.26	8.08×10^{-19}
680	3.5122	-28.81	0.814	5.19×10^{-19}
670	3.5246	-28.54	0.629	3.99×10^{-19}
660	3.5535	-28.21	0.4408	2.78×10^{-19}
650	3.5866	-27.892	0.315	1.98×10^{-19}

CHAPTER 5

CONCLUSIONS

When isothermally aged in the temperature range 520-630K, a Cu-4.9 at% Sb decomposes into a lamellar aggregate of solute rich ε and depleted α phases. The mode of transformation is cellular. The growth rate of the cells increases with temperature at a decreasing rate and starts falling beyond a certain temperature. The interlamellar spacing also increases with increasing aging temperature. Even after 100% transformation, the reaction $\alpha_o \longrightarrow \alpha_{DP} + \varepsilon$ does not undergo completion since the depleted α composition remains slightly higher than that dictated by the equilibrium solvus. The diffusivity values calculated using four different kinetic models are about seven orders of magnitude higher than the volume diffusivity of Sb in Cu. This suggests that solute transport occurs through the grain boundaries. The activation energies are about two-thirds of the value of that for tracer diffusion of Sb in Cu.

Discontinuous dissolution occurs by nucleation and growth of supersaturated α cells at the prior grain boundary positions. The growth rates of dissolution cells, which increase with increasing temperature, are two orders of magnitude higher than that of precipitation cells. The kinetics of discontinuous dissolution has been studied using a model derived from that by Petermann and Hornbogen for discontinuous precipitation. The activation energy obtained from the slope of the linear plot between log $kD_b\delta$ and log 1/T matches well with those estimated for cellular precipitation. This, combined with the higher diffusivity values,

suggests that volume diffusion has an insignificant role to play during the dissolution transformation, which is primarily governed by diffusion of Sb along grain boundaries.

REFERENCES

1. M. Nageswararao, H. Herman, and C. J. McMahon, Jr: Met. Sci, 1976, 10, 249.
2. B. Predel and M. Frebel: Metall. Trans., 1973, 4, 243.
3. L.E. Tanner: Acta Metall., 1972, 20, 1197.
4. E. Hornbogen: Metall. Trans., 1972, 3, 2717.
5. M. N. Thompson: PhD thesis, University of Cambridge, 1971.
6. D. B. Williams and E. P. Butler: Int. Met. Rev., 1981, 3, 153.
7. R. F. Decker and C. T. Sims:'The super-alloys', 57; 1972, New York, Wiley.
8. J. R. Mihalisin and R. F. Decker: Trans. AIME, 1960, 218, 507.
9. S. L. Sass and J. B. Cohen: Trans. AIME, 1969, 245, 153.
10. D. B. Williams and J. W. Edington: Acta Metall., 1976, 24, 323.
11. H. Bohm: Z. Metallk., 1961, 52, 564.
12. V. A. Phillips: Trans. AIME, 1964, 230, 967.
13. G. Meyrick: Scr. Metall., 1976, 10, 649.
14. M. R. Plichta, H. I. Aaronson, J. C. Williams, and G. W. Franti: Scr. Metall., 1979, 13, 407.
15. C. S. Smith: Trans. ASM, 1953, 45, 533.
16. W. Gust, B. Predel, and U. Roll: to be published.
17. K.N. Tu and D. Turnbull: Acta Metall., 1967, 15, 369.
18. R. A. Fournelle and J. B. Clark: Metall. Trans., 1972, 3, 2757.
19. S. P. Gupta and G. T. Parthiban: Metallography, 1988,21, 11.
20. B. E. Sundquist: Met. Trans., 1973, 4, 1919.

21. M. Hillert and R. Lagneborg: J. Mater. Sci., 1971, 6, 208.

22. C. Zener: Trans. AIME, 1946, 167, 550.

23. D. Turnbull: Acta Met., 1955, 3, 55.

24. J. W. Cahn: Acta Met., 1959, 7, 18.

25. M. Hillert, Acta Met., 1982, 30, 1689.

26. J. Petermann and E. Hornbogen, Z. Metallk., 1975, 59, 814.

27. N. Gust, M. B. Hintz, R. Luic and B. Priedel, Met. Res. Soc. Symp. Proc., 1983, 21, 513.

28. S. P. Gupta and V. V. Balasubrahmanyam, Acta Met., 1989, 37, 291.

29. W. Gust and B. Priedel, Met. Trans., 1975, 6A, 1237.

30. L. E. Murr, Interfacial Phen. in Metals and Alloys, Addison Wesley Co., 1975.

31. T. H. Chuang, R. A. Fournelle, W. Gust and B. Predel, Acta Met., 1988, 36, 701.

32. K. Hoshino, Y. Iijima and K. Hirano, Acta Met., 1982, 30, 265.

33. M. C. Inmann and L. W. Barr, Acta Met., 1960, 8. 112.

34. T. J. Renouff, Phil. Mag., 1970, 22, 359.

35. M. S. Sulonen, Acta Met., 1960, 8, 669.

36. R. Nakkalil and S. P. Gupta, Acta Met., 1989, 37, 1903.

37. K. N. Tu and D. Turnbull, Met. Trans., 1971, 2, 2509.

38. A. Pawlowski and W. Truszkowski, Acta Met., 1982, 30, 37.

39. S. P. Gupta, Mater. Sci. Engng., 1976, 84, 255.

40. J. C. Mertz and C. H. Mathewson, Trans. Am. Inst. Min. Engrs, 1937, 124, 59.